

Regional ocean grid refinement and its effect on simulated atmospheric climate

Jonny Williams^{1,*}, Erik Behrens¹, Olaf Morgenstern¹, João Teixeira², Vidya Varma^{1,3}, and Wolfgang Hayek¹

¹*National Institute of Water and Atmospheric Research (NIWA), Hataitai, Wellington, New Zealand*

²*Met Office, Fitzroy Road, EX1 3PB, Exeter, UK*

³*Now at GEOMAR, Düsternbrooker Weg 20, 24105 Kiel, Germany*

**Corresponding author: Jonny Williams, jonny.williams@niwa.co.nz*

July 11, 2023

Abstract

In this work we analyse the impact of including a regional, high-resolution ocean model on simulated atmospheric climate in a coupled earth system model. The resolution of the regional, nested ocean model is approximately 0.2° compared to the 1° resolution of the global ocean model within which it is embedded and this work complements previously published work on ocean circulation and marine heatwaves using the New Zealand Earth System Model, NZESM. After a discussion of the eddy-permitting capability of the nested ocean and its coupling to the overlaying atmosphere, we study the effects on air temperature, precipitation and evaporation, latent and sensible surface heat balances, zonal wind, the storm track and the effect on total cloud amount.

Overall we find that the NZESM provides a better representation of regional atmospheric climate compared to its parent model – UKESM1 – although this improvement is not universal. For example, although the NZESM shows better agreement in surface air temperature within the nested ocean region, there is also some deterioration in the agreement at high southern latitudes where the seasonal sea ice edge coincides with a transition from negative to positive correlation between air temperature and cloud amount. The lack of additional model tuning in the NZESM after the nested ocean model’s inclusion largely accounts for the presence of these improvement-deterioration pairs with respect to observations.

Keywords: Climate, Simulation, Validation

1 Introduction

This paper examines the effect on simulated atmospheric climate of altered ocean physics in a coupled Earth System Model by comparing outputs from a control model, UKESM1-0-LL [1] (‘UKESM1’) and the New Zealand Earth System Model, NZESM [2]. This work is a companion, description paper to previous oceanographic studies [3, 4], focusing on multi-year, annual means. The physical oceanography of the NZESM is described in detail in [3] and the only difference to UKESM1 is the inclusion of an embedded high-resolution ocean model in the New Zealand region, which allows the model to simulate ocean eddies rather than parameterising them.

Climate models’ representations of Southern Ocean climate are subject to some persistent biases in the literature and the Southern Ocean warm bias is one of the best known. What this means in practice is that, in general, climate models do not represent the surface temperature of the Southern Ocean and its overlying atmosphere as well as other regions. The goal of improving our understanding of the climate of the Southern Ocean and Antarctica – New Zealand’s ‘Deep South’ – is the driving goal of the New Zealand Government’s Deep South National

40 Science Challenge, and hence the NZESM itself [2]. The study of Beadling et al. [5] reviews the Southern
 41 Ocean bias in climate models from the 3rd, 5th and 6th Assessment Reports from the Intergovernmental Panel
 42 on Climate Change.

43 Southern Ocean biases in coupled climate models are typically two-fold, manifesting in a persistent surface
 44 warm bias of the Southern Ocean (e.g. [6] §3.1) and in a large shortwave cloud radiative effect - SWCRE - bias
 45 in the overlying atmosphere (e.g. [7] §3). In coupled models these biases are inherently connected, e.g. for the
 46 HadGEM2-ES climate model [8] – the precursor to UKESM1 – results from which were submitted to the 5th
 47 Coupled Model Intercomparison Project (CMIP5) [9]. A detailed discussion of the Southern Ocean biases in
 48 this model can be found elsewhere [10].

49 We focus on changes to (1) air temperature and surface heat flux, (2) the hydrological cycle and (3) westerly
 50 winds and the storm track. The impact of tropical cyclones on New Zealand and mid-latitudes in general is the
 51 subject of a separate in-depth study (Williams et al. 2023, in preparation). The main aim of this work is to act
 52 as a standard reference for future work on the atmospheric climate of the NZESM and related models.

53 2 Models and validation datasets

54 The atmospheric component of the models used here is the ‘Global Atmosphere Model, Version 7.1’ – GA7.1
 55 [11] – configuration of the Unified Model. It uses a semi-implicit semi-Lagrangian dynamical core [12], the
 56 SOCRATES radiation scheme, based on [13], shallow and deep mass-flux-based convection - e.g. [14] - and sub-
 57 gridscale boundary layer turbulence - e.g. [15]. The models also simulate explicit tropospheric and stratospheric
 58 chemistry [16].

59 The ocean model used is NEMO version 3.6 [17], which contains the MEDUSA ocean biogeochemistry
 60 simulator version 2.1 [18] and is coupled to the sea ice model CICE version 5.1.2 [19, 20]. In the nested ocean
 61 model, the ocean diffusivity and viscosity have are different to the global model, the integration time step is
 62 reduced from 2,700s to 900s. The AGRIF formulation is described in detail elsewhere [3].

63 The configuration of the NZESM described here includes a two-way nested, high-resolution ocean model in
 64 the New Zealand region whilst keeping all other aspects of the ocean model unchanged. This nesting has been
 65 achieved using the Adaptive Grid Refinement In Fortran – AGRIF – method [21] and has improved the nominal
 66 ocean grid resolution from 1° to 0.2°, making it ‘eddy permitting’, rather than small-scale eddies needing to be
 67 parameterised. Previous studies using similar ocean model nesting methods have addressed radioactive isotope
 68 dispersal [22] and the ocean circulation of the Agulhas current off southern Africa [23] for example. The study
 69 of Schwarzkopf et al. [24] gives a further example of how this nesting procedure affects model results when a
 70 regional nest with a ‘five to one’ grid mismatch is present, albeit at a significantly higher base resolution.

71 We compare 20-year annual means (1989-2008) of climate model output to observational and reanalysis
 72 products of temperature, precipitation and evaporation, heat fluxes, zonal winds and total cloud amount. The
 73 models runs are started in 1950 to enable model spin-up to occur and both models start from initial conditions
 74 from a UK Met Office simulation [25], which was itself run from 1850. We use data from the ERA5 reanalysis
 75 [26], surface heat flux data from the Objectively Analyzed Air–Sea Heat Fluxes dataset - hereafter ‘OA flux’ -
 76 of [27] and cloud cover from the International Satellite Cloud Climatology project, ISCCP [28, 29].

77 3 Results

78 3.1 Temperature and surface heat balance

79 Figure 1 shows annual mean 1.5m air temperature for UKESM1 and the NZESM compared to the ERA5 re-
 80 analysis [26]. Equivalent sea surface temperature – SST – data is shown in previous work [3]; Figure 1(b) is
 81 analogous to the surface biases shown in Figure 9(a) in [3] and Figures 1(c-d) are analogous to Figures 8(a-b) in
 82 [3]. Note that Figure 9 in [3] shows the mean temperature of the top 500m of the ocean and its Figure 8 shows
 83 the SST.

84 The ocean data in [3] uses the EN4 climatology for sea surface temperature [31] and therefore this serves as
 85 a useful counterpoint to previous analyses with a different ‘ground truth’ dataset.

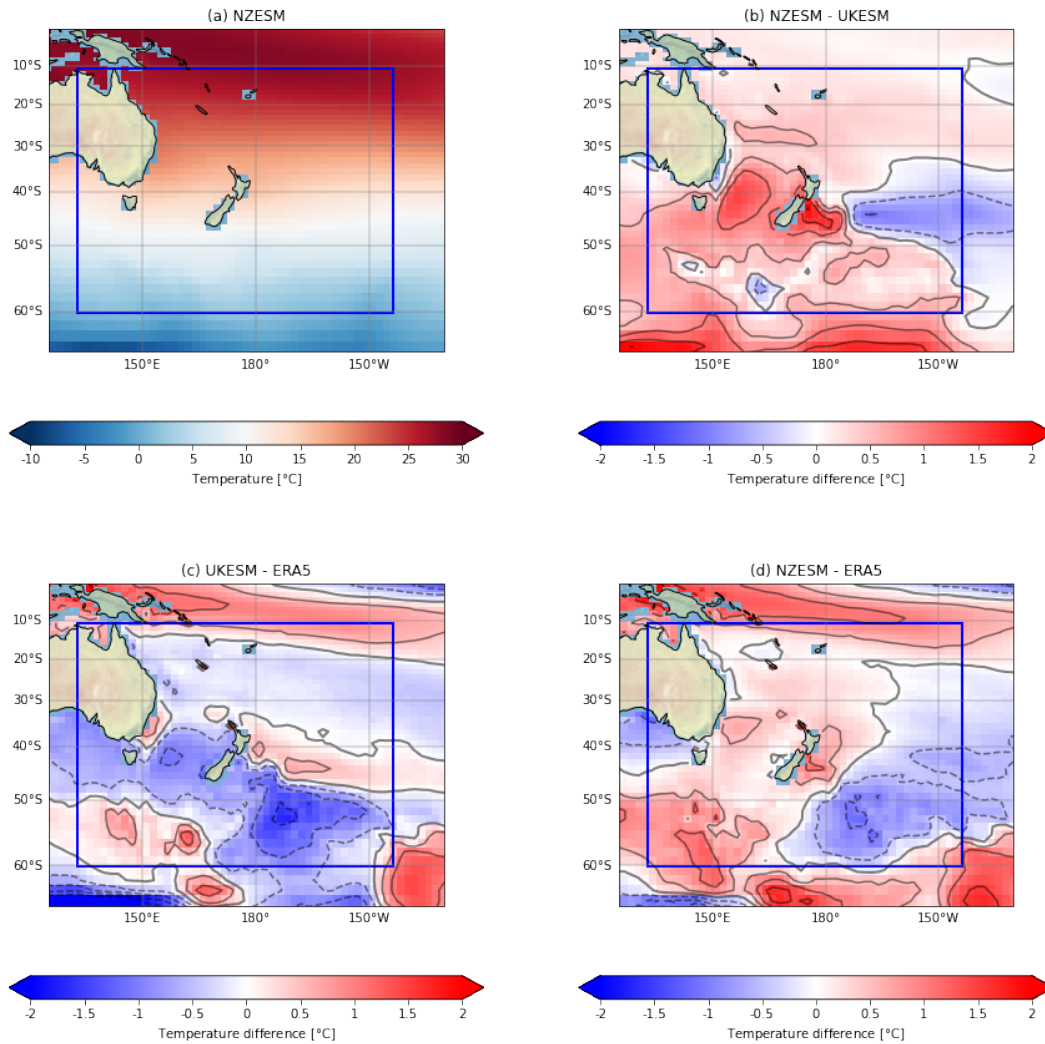


Figure 1: 1.5m annual mean air temperature ($^{\circ}\text{C}$) for: (a) NZESM (b) NZESM - UKESM; (c) NZESM - ERA5 reanalysis; (d) UKESM - ERA5 reanalysis. All data shows annual means for 1989-2008. The region defined by the blue rectangle denotes the location of the high-resolution nested ocean model, i.e. ‘the AGRIF region’, after the method used to implement it [3, 30, 21]. Negative (positive) contours are shown as dashed (solid) lines.

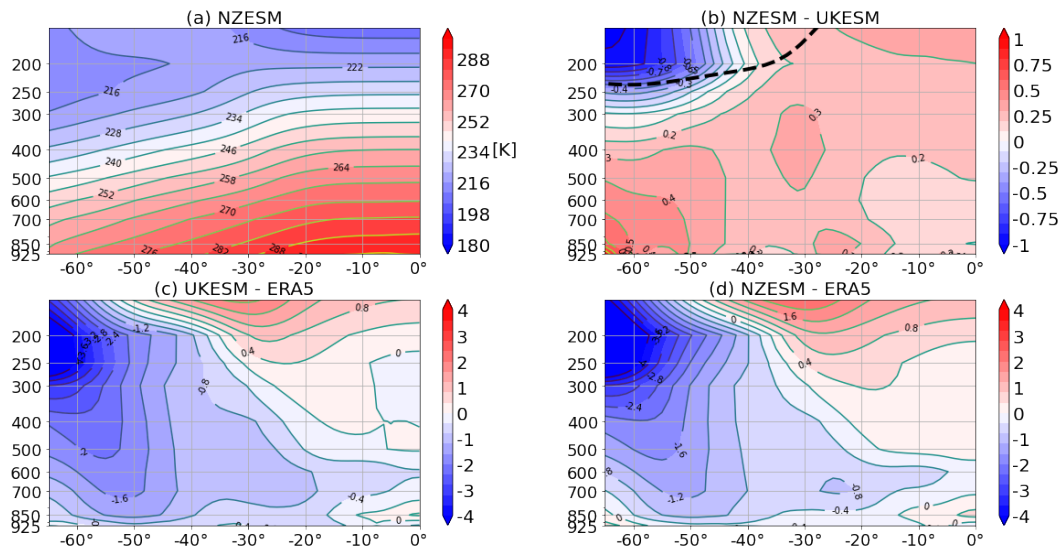


Figure 2: Temperature as a function of pressure: (a) NZESM, (b) NZESM - UKESM, and the NZESM tropopause in this region (c) NZESM - ERA5 reanalysis, (d) UKESM - ERA5 reanalysis. All data is for 1989-2008.

86 Overall, the agreement with the ERA5 reanalysis is better in the NZESM, particularly in the vicinity of the
 87 AGRIF region. However it should be noted that this is not the case universally.

88 The warming seen in the NZESM around -60°S in Figure 1(b) is also visible at even higher southern latitudes.
 89 This is shown later in relation to the effect of the AGRIF region on the storm track, Figure 10(c) where the
 90 NZESM exacerbates the Southern Ocean warm bias already present in UKESM1. Fundamentally, all model
 91 differences shown in this work are due to the inclusion of the nested ocean model since the models are identical
 92 in all other ways. The near-surface temperature fields of the models continue to differ even significantly outside
 93 the extent of the nested model, most notably in the warming of the southern Indian ocean. These ‘far field’
 94 changes can be attributed to ocean circulation changes which increase the southward heat flux in the ocean
 95 which, over time, bring the surface atmosphere into this new, warmer equilibrium state. These changes are
 96 discussed in detail in [3].

97 This combination of a localised improvement accompanied by an associated deterioration elsewhere is often
 98 encountered in climate model development where, e.g., new physical parameterisations are included without any
 99 additional model tuning. The tuning of climate models indeed has its own literature and the interested reader is
 100 referred elsewhere [32, 33, 34].

101 Figure 2 shows zonal mean temperature profiles for the entire region shown in Figure 1.

102 The tropospheric warming signal in the NZESM is clearly visible in Figure 2(b), as is the accompanying
 103 stratospheric cooling, which is expected to achieve overall energy balance [35]. Due to the warming in the
 104 NZESM, the tropopause is raised by up to $\approx 130\text{m}$. This is only $\sim 1\%$ of the total height of the tropopause in
 105 this region, for comparison however, [36] shows that the global warming signal for $20^{\circ}\text{N} - 80^{\circ}\text{N}$ has been ≈ 50
 106 $- 60\text{m}$ per decade for the period 1980-2020.

107 The agreement between the tropospheric temperatures in the NZESM versus the reanalysis data is markedly
 108 improved in the mid-to-lower troposphere. There is some deterioration in the agreement in the stratosphere but
 109 this is of much smaller extent than the formerly mentioned improvement.

110 The general warming observed in the NZESM is primarily due to increased southward heat transport by the
 111 eddy-permitting ocean. This of course not only affects the surface temperature but the structure of the surface
 112 heat balance. Figures 3 and 4 show the surface latent and sensible heat fluxes respectively for the models versus
 113 the OA flux dataset [27].

114 The overall structure of these two figures is - as expected - very similar to temperature response in Figure

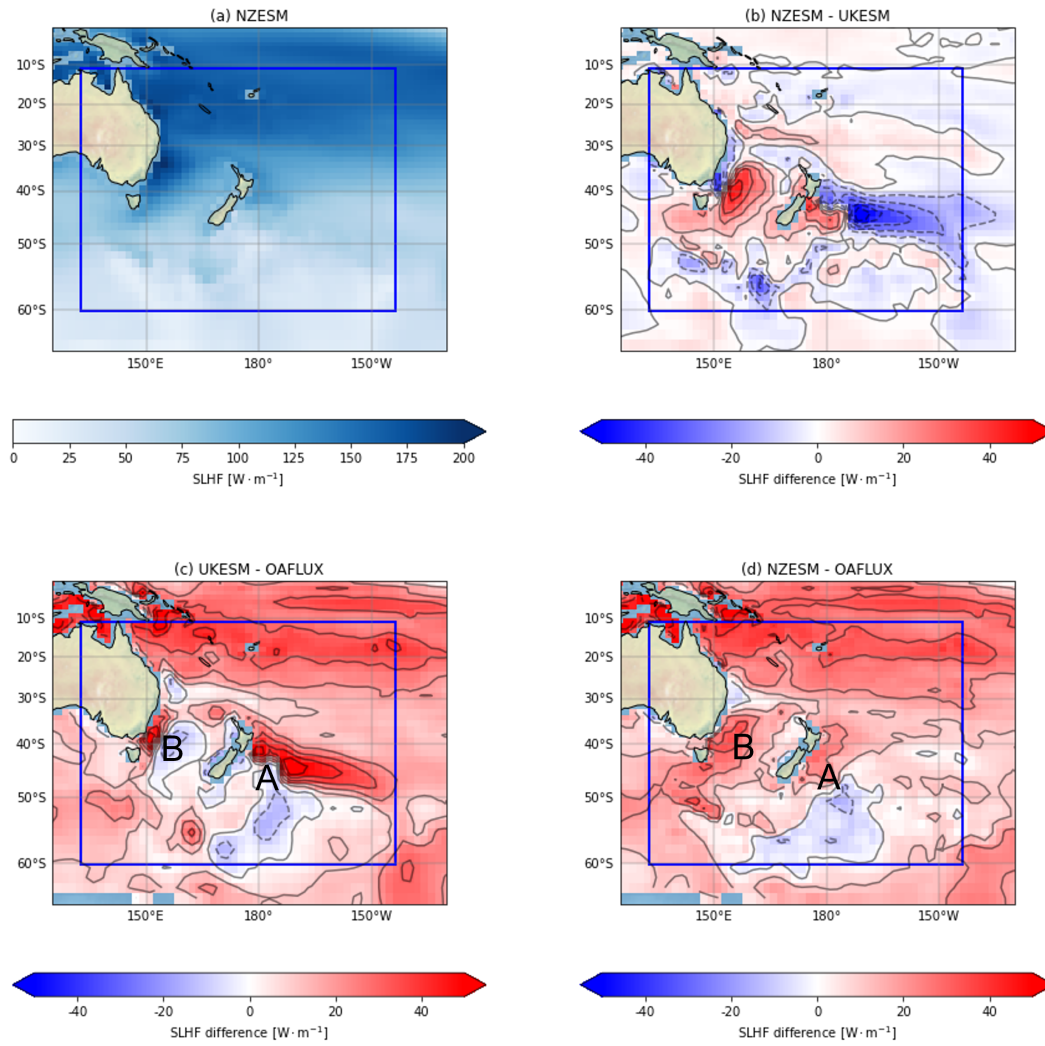


Figure 3: Surface latent heat fluxes ($\text{W} \cdot \text{m}^{-2}$) for the models and with respect to the OA flux dataset [27]. (a) NZESM (b) NZESM - UKESM; (c) NZESM - OA flux; (d) UKESM - OA flux.

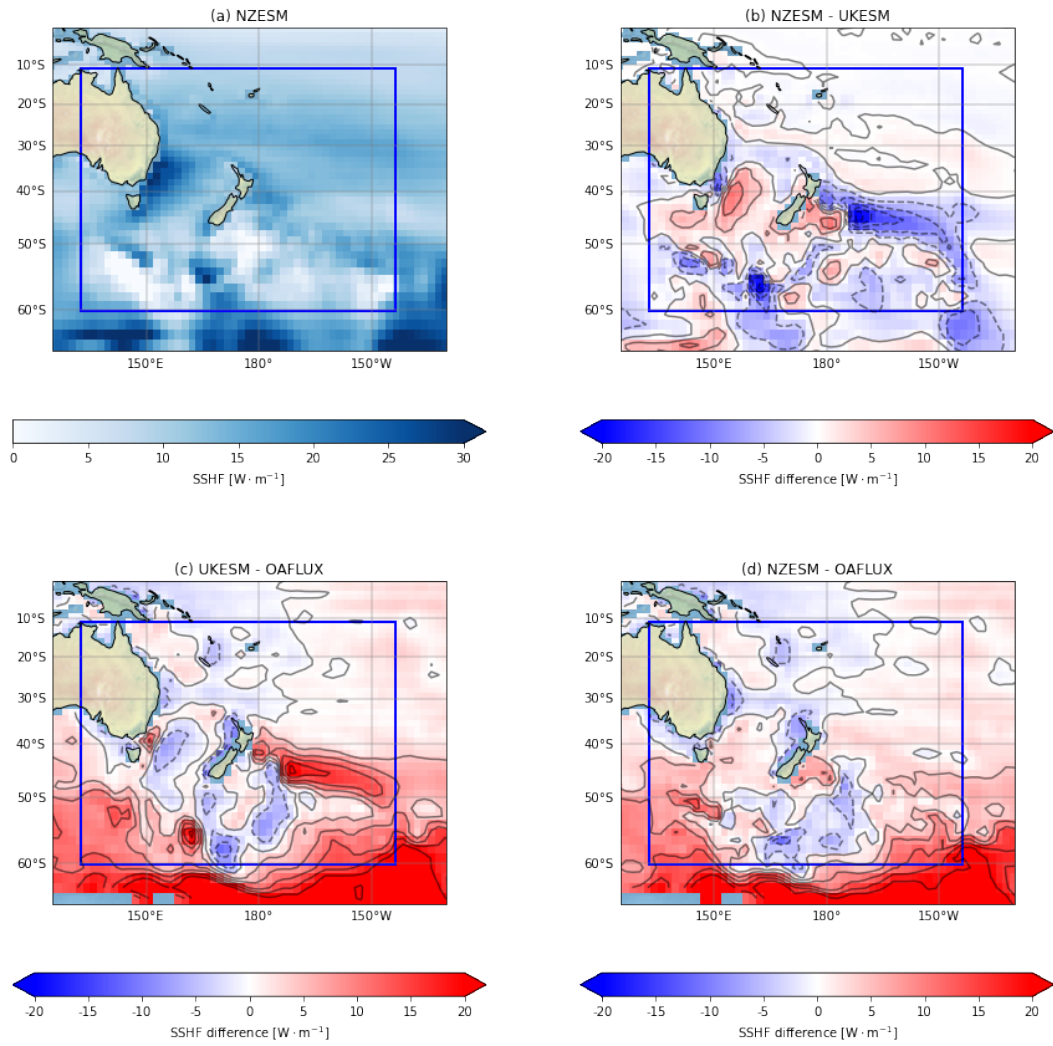


Figure 4: Surface sensible heat fluxes ($\text{W} \cdot \text{m}^{-2}$) for (a) NZESM (b) NZESM - UKESM; (c) NZESM - OA flux; (d) UKESM - OA flux.

115 1. In both cases, the model-data agreement is improved in the NZESM; this is particularly striking in the case
116 of the sensible heating, which shows significantly improved model-reanalysis agreement to the east of New
117 Zealand. The significant positive sensible heat bias in both models at higher southern latitudes (outside the
118 AGRIF region) is indicative of the temperature bias in that region however the agreement within the boundaries
119 of the eddy-permitting ocean is encouraging, illustrating that improved ocean circulation has beneficial effects
120 on atmospheric climate in this coupled framework. In the case of the latent heating there are some areas of
121 improvement (in the region of convergence of the Southland and East Auckland Currents; 'A' in Figure 3(c,d)
122 and deterioration (Tasman Sea and the south east coast of Australia in particular; 'B' in Figure 3(c,d). That said,
123 there is a clear overall improvement in the model-data agreement in Figure 3.

124 3.2 Precipitation, evaporation and cloud amount

125 Moving on to explicitly consider the effect on the hydrological cycle we now look at total precipitation, evapora-
126 tion and cloud amount. Figure 5 shows the annual mean total precipitation fluxes for the models against ERA5
127 reanalysis data.

128 From Figure 5(a) it is clear that by the largest contributor to the total precipitation in this region comes from
129 the South Pacific Convergence Zone – SPCZ – in the northern portion of the Figure 5(a). This region of intense
130 precipitation inclines south-eastwards from the Maritime Continent and shows a southward trend in the NZESM
131 . This is evidenced by drying in the northern portion and moistening in the southern portion in the northeast of
132 Figure 5(b). This sub-figure also shows a general drying to the east and a moistening to the west of New Zealand,
133 which is anti-correlated to the 1.5m temperature changes observed in Figure 1(b).

134 Comparing Figures 5(c) and (d) we see that the NZESM reduces both wet and dry biases close to New
135 Zealand and that the southward shift of the SPCZ is evident in the more concentrated drying signal in Figure
136 5(d) with respect to ERA5.

137 Figures 6 and 7 show sea to air evaporation flux and precipitation minus evaporation ($P - E$) for the models
138 and ERA5 respectively.

139 Overall, the pattern of changes in the evaporation are of the same sign as the precipitation. That is, regions
140 which show more precipitation also show more evaporation, and vice versa. However, the changes to the evapora-
141 tion flux are generally larger than the changes to precipitation and hence the region to the east of New Zealand
142 shows positive $P - E$ change even though the amount of precipitation in this region is decreased. The sign of
143 this effect is reversed over the Tasman Sea which shows an overall ‘drying’ – negative $\Delta(P - E)$ – in spite of
144 increasing precipitation.

145 Now considering total cloud amount, Figure 8(b) shows that there is a general increase in cloud in the NZESM
146 to the east of New Zealand . The reverse seen in the SPCZ and around the Tasman Sea. At mid-latitudes, the
147 sign of this change is anti-correlated with the temperature change – Figure 1(b) – and in the SPCZ there is a
148 clear relationship between the reduction in total cloud and the amount of precipitation, Figure 5(b). At higher
149 latitudes, the sign of the relationship between increasing temperature and cloud cover is reversed and there is
150 clear increase in total cloud amount in the vicinity of the maximum sea ice extent. The sea ice edges shown in
151 Figure 8(b-d) are the 15% contours of the September (i.e. the maximum) sea ice extent from the 20 years of
152 model data considered for both models. This is a prognostic output from the CICE model which is identical in
153 the two models.

154 Due to the warming in the NZESM around -60° , the sea ice retreats southward and allows increased potential-
155 evaporation from the ocean surface, thus favouring increased cloud cover. This complex behaviour illustrates the
156 utility of using a coupled climate model to study ocean-ice-atmosphere interactions since in an atmosphere-only
157 climate model configuration, the relationship between sea ice retreat and cloud cover could not be examined at
158 all.

159 These intra-model differences notwithstanding, the differences between the models and the observations
160 are an order of magnitude larger, Figure 8(c,d). Therefore the changes made in the NZESM do not make any
161 notable difference to the overall agreement between the models and observations and hence significant model-
162 observation disagreement remains.

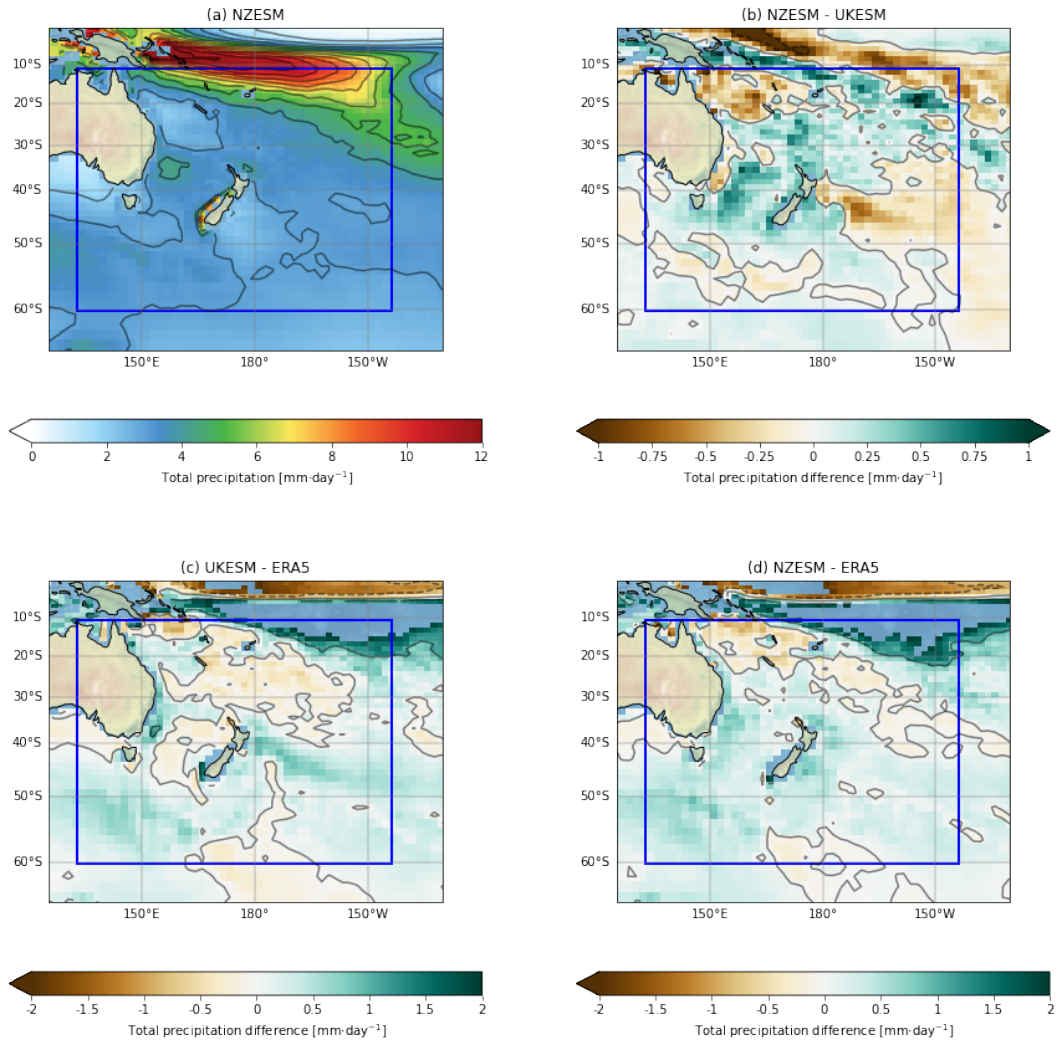


Figure 5: Total precipitation ($\text{mm} \cdot \text{day}^{-1}$) for (a) NZESM, (b) NZESM - UKESM, (c) UKESM - ERA5, (d) NZESM - ERA5. Contour levels for levels for all plots are at integer values and for (c) and (d) values over $2 \text{mm} \cdot \text{day}^{-1}$ are masked to aid visual interpretation.

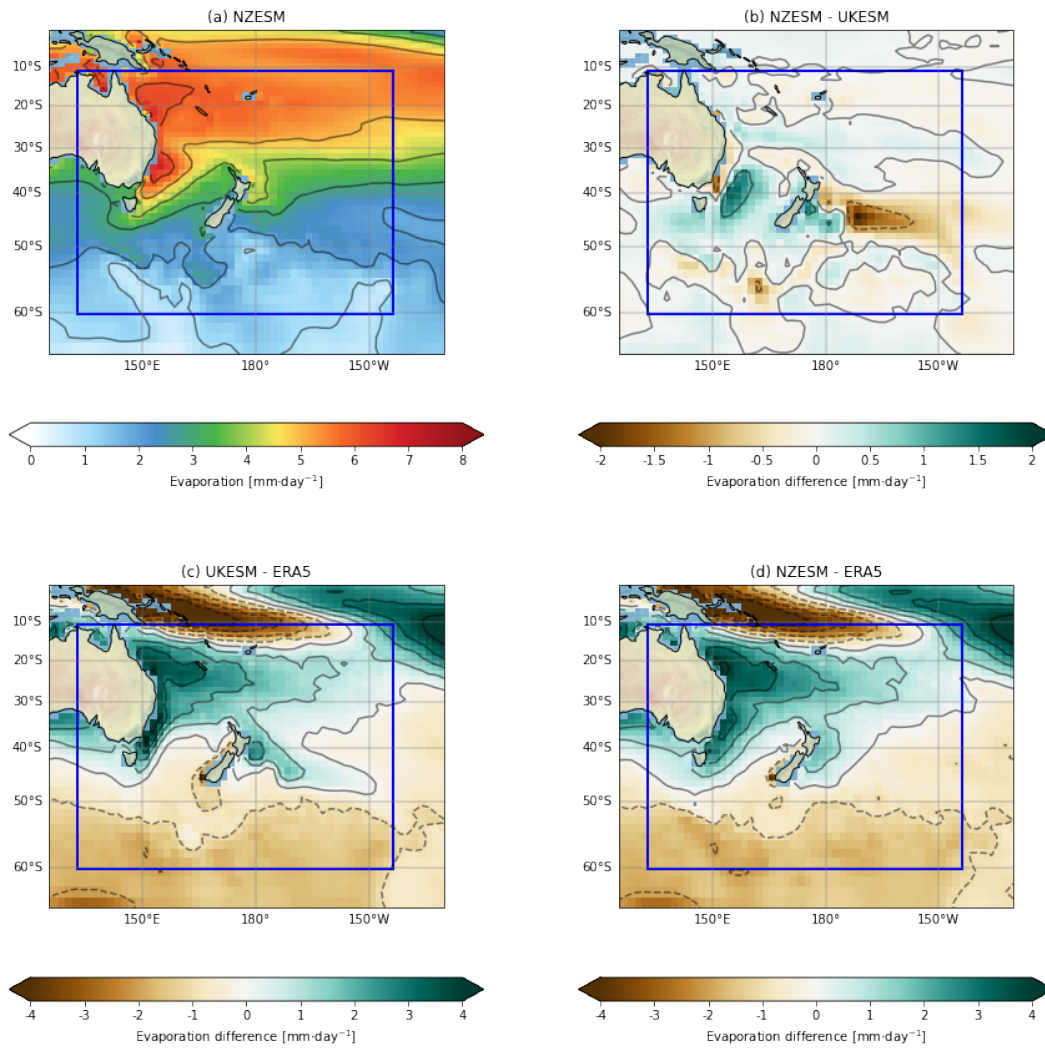


Figure 6: Sea to air evaporation ($\text{mm} \cdot \text{day}^{-1}$) for (a) NZESM, (b) NZESM - UKESM, (c) UKESM - ERA5, (d) NZESM - ERA5. Contour levels for levels for all plots are at integer values.

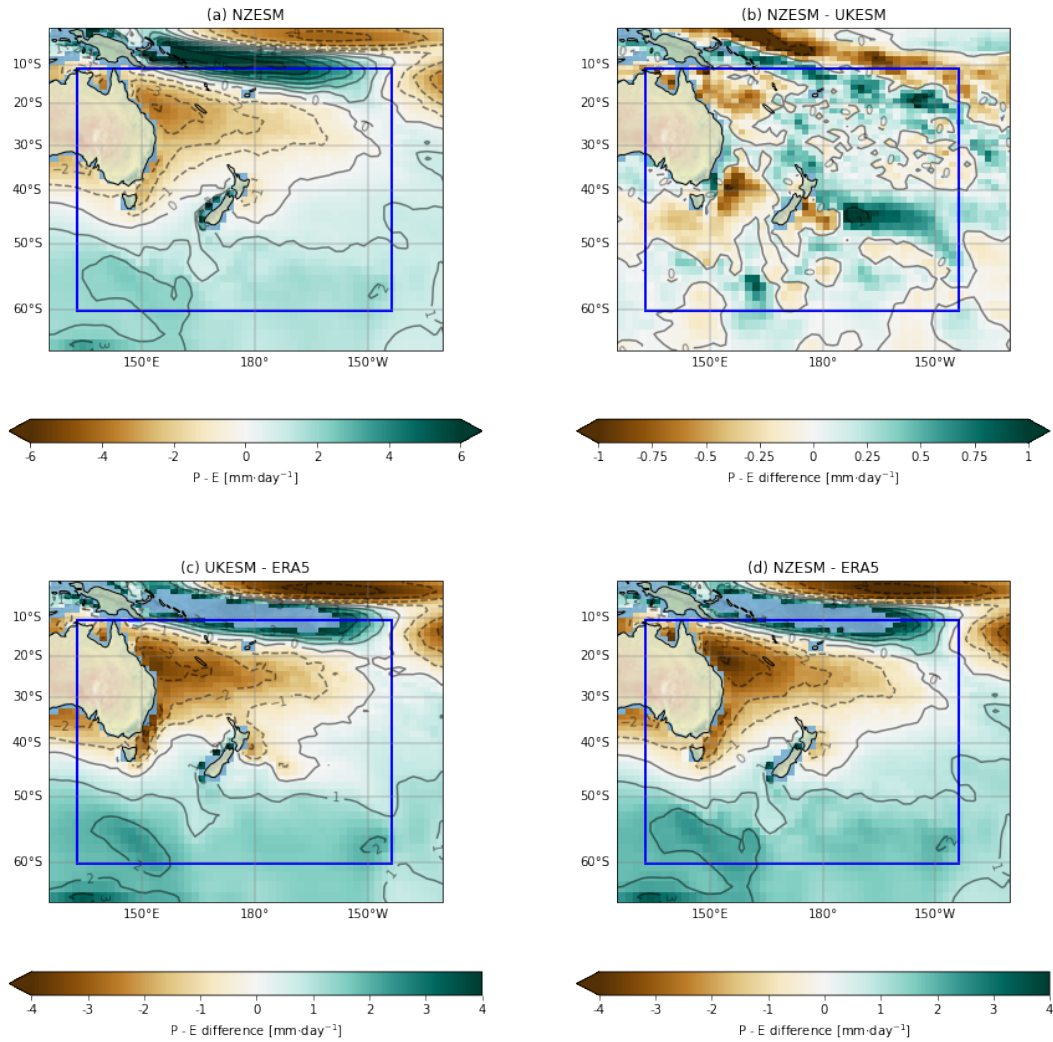


Figure 7: $P - E$ ($\text{mm} \cdot \text{day}^{-1}$) for (a) NZESM, (b) NZESM - UKESM, (c) UKESM - ERA5, (d) NZESM - ERA5. Contour levels for levels for all plots are at integer values and for (c) and (d) values over $4 \text{ mm} \cdot \text{day}^{-1}$ are masked to aid visual interpretation.

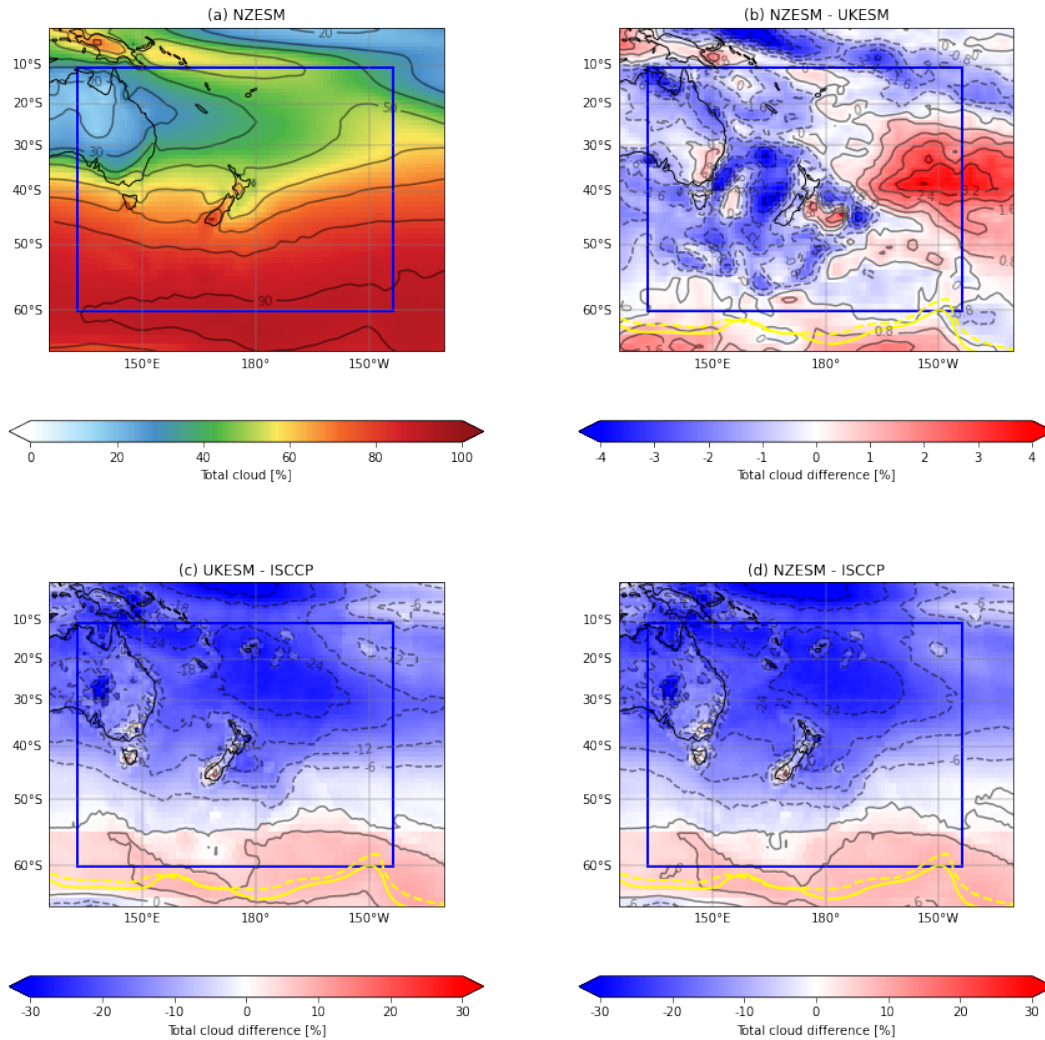


Figure 8: Total cloud for (a) NZESM observations, (b) NZESM - UKESM, (c) UKESM - observations, (d) NZESM - observations. Figure (b-d) show 15% contours of September sea ice cover for UKESM1 (dashed line) and the NZESM (solid line), which is a commonly-used measure of sea ice extent [37]. Observed cloud amount data is from the International Satellite Cloud Climatology Project, ISCCP [28].

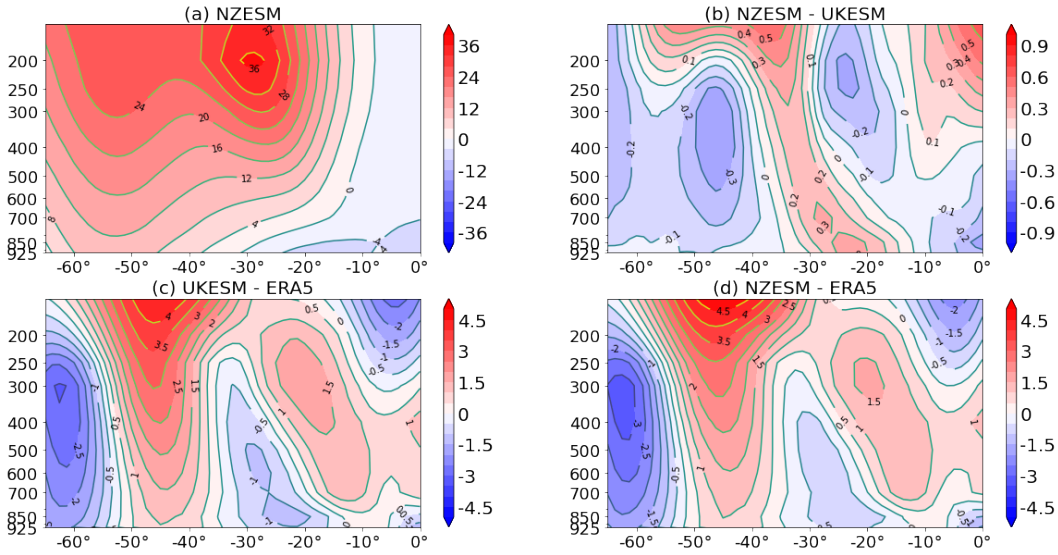


Figure 9: Zonal mean zonal wind ($\text{m} \cdot \text{s}^{-1}$) for: (a) NZESM (b) NZESM - UKESM; (c) NZESM - ERA5 reanalysis; (d) UKESM - ERA5 reanalysis.

163 3.3 Zonal wind and the storm track

164 New Zealand’s climate is primarily maritime-driven, and the prevailing westerlies are a key driver of West Coast
 165 rainfall [38]. Before examining the position of the storm track, we study the zonal component of the wind. Figure
 166 9 shows this for same the region considered above.

167 In Figure 9(a) the dominance of the westerlies is clearly visible in the mostly-positive sign of u and the jet is
 168 clearly visible at around 200hPa and $\approx 30^\circ\text{S}$.

169 Figure 9(b) shows that there is a small but non-negligible southward shift of the jet in the NZESM and (c), (d)
 170 show a general improvement in model-reanalysis agreement, particularly at latitudes north of $\approx -30^\circ\text{S}$. This is
 171 a further illustration of the utility of how using a higher-resolution ocean can have ‘downstream’ improvements
 172 in model physics.

173 Using the stormTracking package (<https://github.com/ecjoliver/stormTracking>) we have gen-
 174 erated maps of the number of unique cyclones - N_c - in 6-hourly mean sea level pressure data, Figure 10.

175 Figure 10 shows two main features of the N_c distribution in the NZESM :

- 176 1. A general weakening of the storm storm track at latitudes affecting New Zealand, around 30-50°S.
- 177 2. Strengthening at higher latitudes, particularly to the north and east of the Ross Sea.

178 What these changes amount to is a general southerly movement of the storm track and this is particularly
 179 evident to the east of New Zealand. Comparing this behaviour with Figure 10(c) shows that there is a general
 180 relationship between SST and storm activity; the decrease in SST to the east of NZ for example is accompanied
 181 by a concomitant decrease in storm activity. We also see a correspondence south of -60° where the increase in
 182 SST is accompanied by an increase in storminess. Although this relationship appears to apply on large spatial
 183 scales, it is not universal. For example, Figure 1 shows an increase in the SST in the immediate vicinity of NZ
 184 whilst the storminess shows some evidence of decreasing. This behaviour however is somewhat isolated and is
 185 may due to land-sea heat capacity contrast. A more detailed exploration of the models’ storm climatologies and
 186 how they are predicted to change over the course of the 21st century is the subject of ongoing research and will
 187 be published elsewhere.

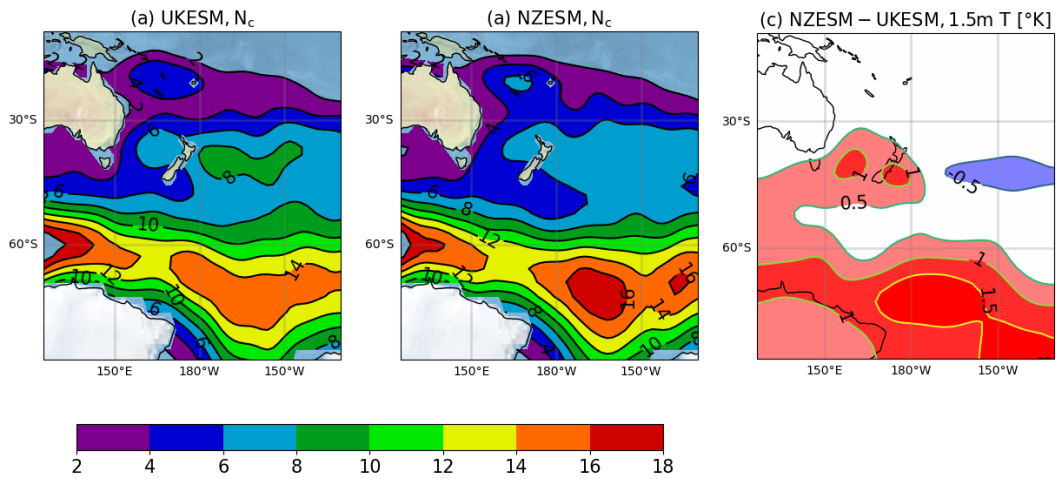


Figure 10: (a) UKESM N_c , (b) NZESM N_c , (c) NZESM - UKESM 1.5m air temperature difference; all with $\sigma = 2$ in the Gaussian smoothing calculations. The data in (a), (b) is obtained from the `stormTracking` software and uses the mesoscale feature tracking capability described in [39] by firstly identifying and then following each individual system through time. The number of unique cyclone tracks in each gridbox are then counted in each grid box and smoothed using a Gaussian kernel standard deviation of 2 in the `SciPy` software [40]. Without this additional smoothing the data are too noisy to enable a reasonable interpretation of the differences between the datasets and since the smoothing reduces the absolute value of N_c , the numerical values of the contours are somewhat arbitrary. As a rough guide, the $\sigma = 2$ smoothing reduces the raw N_c values by approximately a factor of 2. The data in (c) is the same as in Figure 1(b) with a southward extension to better illustrate the relationship with the storm track.

4 Conclusions

In this work we have studied the regional atmospheric climate of two historical simulations of the period 1989 - 2008 using configurations of UKESM1 model with [3] and without [41, 1] a nested, regional ocean model, the introduction of which improves several aspects of model-observation agreement. We have split the analysis into three sections. Firstly we examined the air temperature at the surface and aloft and how this affects surface heat balance. Next, the hydrological response, and finally the effect on the westerly wind structure and the storm track.

The 1.5m air temperature closely mirrors the improvements seen in the equivalent plots shown in [3]. This is of course expected since the data presented are multi-decadal annual means for the same model pair. Above the boundary layer, the NZESM exhibits tropospheric warming and stratospheric cooling, the former of which leads to a significant improvement in model-reanalysis agreement and a raising of the tropopause height by a comparable amount to the climate change signal over recent decades. The surface heat balance in the NZESM is improved with respect to observations and this is particularly striking for the latter. In common with virtually all model development changes the observed changes are not all beneficial, Overall however, the improvements are beneficial to model performance, even in the absence of additional model tuning.

The SPCZ dominates the precipitation signal and shows a southward shift in the NZESM. The NZESM also shows reduced wet and dry biases close to New Zealand. Evaporation changes are generally of the same sign as the precipitation changes, but larger in magnitude, meaning that $\Delta(P - E)$ is of the opposite sign to ΔP in some areas. The first-order effect of the NZESM's high-resolution ocean is to increase total cloud cover to the east of New Zealand and to decrease it over the Tasman sea and the SPCZ. These cloud changes are generally anti-correlated with surface temperature changes at mid-latitudes, but the reverse is seen at high latitudes near the seasonal sea ice edge.

The structure of the westerly winds shows some improvement in the NZESM and the storm track is shifted south which mirrors the general warming signal introduced by the high-resolution ocean. Future work using this nesting methodology on other similarly-related model pairs, as well as this same model pair in different regions would be of significant interest. Additionally, nesting of a high-resolution atmosphere within the global, coupled model would complement the longstanding history of regional atmosphere modelling in New Zealand, e.g. [42].

A NZESM runtime configuration

Given the significant computational expense of Earth System Models, it is very important to optimise the build and runtime configuration of the component model executables to achieve best efficiency. Ideal setups depend on the characteristics of the target high-performance computing (HPC) platform, such as the number of CPU cores per node, CPU architecture, choice of compilers and libraries, as well as the interconnect that is used for communicating data between the processes that run the model in parallel, and the storage system.

NZESM consists of separate executables for the atmosphere (Unified Model) and ocean (NEMO) components, which are coupled using the OASIS library. CPU cores on the HPC need to be distributed between these components to match their respective runtime between data exchanges as closely as possible, as any wait times will reduce efficiency. With the atmosphere model requiring many more cores than the ocean model to handle its much larger computational expense, just enough resources should be assigned to the ocean so that the atmosphere does not need to wait for data to arrive. OASIS comes with a timing feature to help find the right balance.

The Unified Model and NEMO use the Message Passing Library (MPI) for distributed parallel computing, where finding an optimal CPU core count for a given science configuration typically involves trade-offs between runtime and computational efficiency ("strong scaling"). While assigning more cores will speed up computation and thus achieve a higher number of model years per wall clock time interval, communication overheads become more and more important with increasing core count and reduce computational efficiency, as relatively more time needs to be spent on non-science related computation. It is usually advisable to start with a minimum number of cores that allows the model to meet runtime expectations at reasonable efficiency, especially on a busy HPC, where smaller core counts can lead to shorter queuing times and thus higher overall throughput. If

236 communication overhead is still small and if there is enough capacity on the HPC, core counts can be increased
237 to reduce runtime without suffering much efficiency loss ("linear scaling").

238 Both the Unified Model and NEMO impose constraints on how CPU cores can be used for parallel computing
239 with the "domain decomposition" approach, which can prevent configurations from using all available cores on
240 the assigned HPC nodes and thus impact efficient resource utilisation.

241 The Māui HPC that was used for this work comes with 40 Intel Skylake CPU cores per node. The original
242 core count configuration of NZESM was readjusted for Māui to minimise atmosphere/ocean runtime imbalance,
243 minimise the number of unused cores on the nodes, and maximise MPI parallelisation efficiency. This led to a
244 28% node count reduction from 32 nodes to 23 with only a modest 5% increase in runtime from 7.7 hours per
245 model year to 8.1 hours per model year. Overall computational resource utilisation by NZESM was thus reduced
246 by 24%.

247 Acknowledgements

248 This paper obtained funding and support through the Ministry of Business Innovation and Employment Deep
249 South National Science Challenge projects (C01X1412) and Royal Society Marsden Fund (NIW1701). The
250 development of UKESM1, was supported by the Met Office Hadley Centre Climate Programme funded by
251 BEIS and Defra (GA01101) and by the Natural Environment Research Council (NERC) national capability
252 grant for the UK Earth System Modelling project, grant number NE/N017951/1. The authors would also
253 like to acknowledge the support and collaboration of the wider Unified Model Partnership, [https://www.
254 metoffice.gov.uk/research/approach/collaboration/unified-model/partnership](https://www.metoffice.gov.uk/research/approach/collaboration/unified-model/partnership). and the use
255 of New Zealand eScience Infrastructure (NeSI) high performance computing facilities, consulting support and
256 training services as part of this research. New Zealand's national facilities are provided by NeSI and funded
257 jointly by NeSI's collaborator institutions and through the Ministry of Business, Innovation & Employment's
258 Research Infrastructure programme, www.nesi.org.nz. The ocean and sea ice code used in this work is avail-
259 able online at <https://doi.org/10.5281/zenodo.3873691>. The model output of the NZESM (u-b1274
260 Met Office identifier) and UKESM (u-bm456 Met Office identifier) used for the manuscript is publicly avail-
261 able via Zenodo (<https://doi.org/10.5281/zenodo.6534266>). ERA5 data is publicly available from
262 <https://www.ecmwf.int/en/forecasts/datasets/reanalysis-datasets/era5>.

263 References

- 264 [1] Alistair A. Sellar et al. "Implementation of U.K. Earth System Models for CMIP6". In: *Journal of Ad-
265 vances in Modeling Earth Systems* 12.4 (2020). e2019MS001946 10.1029/2019MS001946, e2019MS001946.
266 DOI: <https://doi.org/10.1029/2019MS001946>.
- 267 [2] J. Williams et al. "Development of the New Zealand Earth System Model: NZESM". In: *Weather and
268 Climate* 36 (2016), pp. 25–44. ISSN: 01115499.
- 269 [3] Erik Behrens et al. "Local Grid Refinement in New Zealand's Earth System Model: Tasman Sea Ocean
270 Circulation Improvements and Super-Gyre Circulation Implications". In: *Journal of Advances in Mod-
271 eling Earth Systems* 12.7 (2020). e2019MS001996 2019MS001996, e2019MS001996. DOI: [https://
272 doi.org/10.1029/2019MS001996](https://doi.org/10.1029/2019MS001996).
- 273 [4] Erik Behrens et al. "Projections of future marine heatwaves for the oceans around New Zealand using
274 New Zealand's earth system model". In: *Frontiers in Climate* 4 (2022), p. 798287.
- 275 [5] R. L. Beadling et al. "Representation of Southern Ocean Properties across Coupled Model Intercompar-
276 ison Project Generations: CMIP3 to CMIP6". In: *Journal of Climate* 33.15 (2020), pp. 6555–6581. DOI:
277 <https://doi.org/10.1175/JCLI-D-19-0970.1>.
- 278 [6] A. Yool et al. "Evaluating the physical and biogeochemical state of the global ocean component of
279 UKESM1 in CMIP6 historical simulations". In: *Geoscientific Model Development* 14.6 (2021), pp. 3437–
280 3472. DOI: [10.5194/gmd-14-3437-2021](https://doi.org/10.5194/gmd-14-3437-2021).

- 281 [7] Vidya Varma et al. “Improving the Southern Ocean cloud albedo biases in a general circulation model”.
282 In: *Atmospheric Chemistry and Physics* 20.13 (July 2020), pp. 7741–7751. DOI: [10.5194/acp-20-](https://doi.org/10.5194/acp-20-7741-2020)
283 [7741-2020](https://doi.org/10.5194/acp-20-7741-2020).
- 284 [8] Matt Hawcroft et al. “Southern Ocean albedo, inter-hemispheric energy transports and the double ITCZ:
285 global impacts of biases in a coupled model”. In: *Climate Dynamics* 48.7-8 (June 2016), pp. 2279–2295.
286 DOI: [10.1007/s00382-016-3205-5](https://doi.org/10.1007/s00382-016-3205-5).
- 287 [9] Karl E Taylor, Ronald J Stouffer, and Gerald A Meehl. “An overview of CMIP5 and the experiment
288 design”. In: *Bulletin of the American meteorological Society* 93.4 (2012), pp. 485–498.
- 289 [10] Baijun Tian and Xinyu Dong. “The double-ITCZ bias in CMIP3, CMIP5, and CMIP6 models based on
290 annual mean precipitation”. In: *Geophysical Research Letters* 47.8 (2020), e2020GL087232.
- 291 [11] David Walters et al. “The Met Office Unified Model global atmosphere 7.0/7.1 and JULES global land
292 7.0 configurations”. In: *Geoscientific Model Development* 12.5 (2019), pp. 1909–1963.
- 293 [12] Nigel Wood et al. “An inherently mass-conserving semi-implicit semi-Lagrangian discretization of the
294 deep-atmosphere global non-hydrostatic equations”. In: *Quarterly Journal of the Royal Meteorological*
295 *Society* 140.682 (2014), pp. 1505–1520. DOI: <https://doi.org/10.1002/qj.2235>.
- 296 [13] J. M. Edwards and A. Slingo. “Studies with a flexible new radiation code. I: Choosing a configuration for
297 a large-scale model”. In: *Quarterly Journal of the Royal Meteorological Society* 122.531 (1996), pp. 689–
298 719. DOI: <https://doi.org/10.1002/qj.49712253107>.
- 299 [14] D. Gregory and P. R. Rowntree. “A Mass Flux Convection Scheme with Representation of Cloud En-
300 semble Characteristics and Stability-Dependent Closure”. In: *Monthly Weather Review* 118.7 (1990),
301 pp. 1483–1506. DOI: [10.1175/1520-0493\(1990\)118<1483:AMFCSW>2.0.CO;2](https://doi.org/10.1175/1520-0493(1990)118<1483:AMFCSW>2.0.CO;2).
- 302 [15] AR Brown et al. “Upgrades to the boundary-layer scheme in the Met Office numerical weather prediction
303 model”. In: *Boundary-Layer Meteorology* 128.1 (2008), pp. 117–132.
- 304 [16] A. T. Archibald et al. “Description and evaluation of the UKCA stratosphere–troposphere chemistry
305 scheme (StratTrop v1.0) implemented in UKESM1”. In: *Geoscientific Model Development* 13.3 (2020),
306 pp. 1223–1266. DOI: [10.5194/gmd-13-1223-2020](https://doi.org/10.5194/gmd-13-1223-2020).
- 307 [17] Madec Gurvan et al. *NEMO ocean engine*. Version v4.2. Mar. 2022. DOI: [10.5281/zenodo.6334656](https://doi.org/10.5281/zenodo.6334656).
308 URL: <https://doi.org/10.5281/zenodo.6334656>.
- 309 [18] A. Yool, E. E. Popova, and T. R. Anderson. “MEDUSA-2.0: an intermediate complexity biogeochemical
310 model of the marine carbon cycle for climate change and ocean acidification studies”. In: *Geoscientific*
311 *Model Development* 6.5 (2013), pp. 1767–1811. DOI: [10.5194/gmd-6-1767-2013](https://doi.org/10.5194/gmd-6-1767-2013).
- 312 [19] Elizabeth Hunke et al. *CICE, The Los Alamos Sea Ice Model, Version 00*. May 2017.
- 313 [20] Jeff K Ridley et al. “The sea ice model component of HadGEM3-GC3. 1”. In: *Geoscientific Model De-*
314 *velopment* 11.2 (2018), pp. 713–723.
- 315 [21] Laurent Debreu, Christophe Vouland, and Eric Blayo. “AGRIF: Adaptive grid refinement in Fortran”. In:
316 *Computers & Geosciences* 34.1 (2008), pp. 8–13.
- 317 [22] Erik Behrens et al. “Model simulations on the long-term dispersal of 137Cs released into the Pacific Ocean
318 off Fukushima”. In: *Environmental Research Letters* 7.3 (July 2012), p. 034004. DOI: [10.1088/1748-](https://doi.org/10.1088/1748-9326/7/3/034004)
319 [9326/7/3/034004](https://doi.org/10.1088/1748-9326/7/3/034004).
- 320 [23] Arne Biastoch, Claus W Böning, and JRE Lutjeharms. “Agulhas leakage dynamics affects decadal vari-
321 ability in Atlantic overturning circulation”. In: *Nature* 456.7221 (2008), pp. 489–492.
- 322 [24] F. U. Schwarzkopf et al. “The INALT family – a set of high-resolution nests for the Agulhas Current
323 system within global NEMO ocean/sea-ice configurations”. In: *Geoscientific Model Development* 12.7
324 (2019), pp. 3329–3355. DOI: [10.5194/gmd-12-3329-2019](https://doi.org/10.5194/gmd-12-3329-2019).
- 325 [25] Yongming Tang et al. *MOHC UKESM1.0-LL model output prepared for CMIP6 CMIP historical*. 2019.
326 DOI: [10.22033/ESGF/CMIP6.6113](https://doi.org/10.22033/ESGF/CMIP6.6113).

- 327 [26] Hans Hersbach et al. “The ERA5 global reanalysis”. In: *Quarterly Journal of the Royal Meteorological*
328 *Society* 146.730 (2020), pp. 1999–2049.
- 329 [27] Lisan Yu and Robert A. Weller. “Objectively Analyzed Air–Sea Heat Fluxes for the Global Ice-Free
330 Oceans (1981–2005)”. In: *Bulletin of the American Meteorological Society* 88.4 (2007), pp. 527–540.
331 DOI: [10.1175/BAMS-88-4-527](https://doi.org/10.1175/BAMS-88-4-527).
- 332 [28] William B Rossow and Robert A Schiffer. “Advances in understanding clouds from ISCCP”. In: *Bulletin*
333 *of the American Meteorological Society* 80.11 (1999), pp. 2261–2288.
- 334 [29] WB Rossow and EN Duenas. “The international satellite cloud climatology project (ISCCP) web site: An
335 online resource for research”. In: *Bulletin of the American Meteorological Society* 85.2 (2004), pp. 167–
336 172.
- 337 [30] Erik Behrens. *erikbehrens/NZESM1: First release of the NZESM (ocean+sea ice code)*. Version v1.0.
338 2020. DOI: [10.5281/zenodo.3873691](https://doi.org/10.5281/zenodo.3873691). URL: <https://doi.org/10.5281/zenodo.3873691>.
- 339 [31] Simon A Good, Matthew J Martin, and Nick A Rayner. “EN4: Quality controlled ocean temperature and
340 salinity profiles and monthly objective analyses with uncertainty estimates”. In: *Journal of Geophysical*
341 *Research: Oceans* 118.12 (2013), pp. 6704–6716.
- 342 [32] Gavin A. Schmidt et al. “Practice and philosophy of climate model tuning across six US modeling centers”.
343 In: *Geoscientific Model Development* 10.9 (Sept. 2017), pp. 3207–3223. DOI: [10.5194/gmd-10-3207-](https://doi.org/10.5194/gmd-10-3207-2017)
344 [2017](https://doi.org/10.5194/gmd-10-3207-2017).
- 345 [33] Frédéric Hourdin et al. “The Art and Science of Climate Model Tuning”. In: *Bulletin of the American*
346 *Meteorological Society* 98.3 (Mar. 2017), pp. 589–602. DOI: [10.1175/bams-d-15-00135.1](https://doi.org/10.1175/bams-d-15-00135.1).
- 347 [34] Doug McNeall et al. “Correcting a bias in a climate model with an augmented emulator”. In: *Geoscientific*
348 *Model Development* 13.5 (May 2020), pp. 2487–2509. DOI: [10.5194/gmd-13-2487-2020](https://doi.org/10.5194/gmd-13-2487-2020).
- 349 [35] Petr Pisoft et al. “Stratospheric contraction caused by increasing greenhouse gases”. In: *Environmental*
350 *Research Letters* 16.6 (May 2021), p. 064038. DOI: [10.1088/1748-9326/abfe2b](https://doi.org/10.1088/1748-9326/abfe2b).
- 351 [36] Lingyun Meng et al. “Continuous rise of the tropopause in the Northern Hemisphere over 1980–2020”.
352 In: *Science Advances* 7.45 (2021), eabi8065. DOI: [10.1126/sciadv.abi8065](https://doi.org/10.1126/sciadv.abi8065).
- 353 [37] R. Kwok and D. A. Rothrock. “Decline in Arctic sea ice thickness from submarine and ICESat records:
354 1958–2008”. In: *Geophysical Research Letters* 36.15 (2009). DOI: [https://doi.org/10.1029/](https://doi.org/10.1029/2009GL039035)
355 [2009GL039035](https://doi.org/10.1029/2009GL039035).
- 356 [38] Kimberley J Reid et al. “Extreme rainfall in New Zealand and its association with Atmospheric Rivers”.
357 In: *Environmental Research Letters* 16.4 (Mar. 2021), p. 044012. DOI: [10.1088/1748-9326/abeae0](https://doi.org/10.1088/1748-9326/abeae0).
- 358 [39] Dudley B. Chelton, Michael G. Schlax, and Roger M. Samelson. “Global observations of nonlinear
359 mesoscale eddies”. In: *Progress in Oceanography* 91.2 (2011), pp. 167–216. ISSN: 0079-6611. DOI: <https://doi.org/10.1016/j.pocean.2011.01.002>.
- 360
- 361 [40] Pauli Virtanen et al. “SciPy 1.0: Fundamental Algorithms for Scientific Computing in Python”. In: *Nature*
362 *Methods* 17 (2020), pp. 261–272. DOI: [10.1038/s41592-019-0686-2](https://doi.org/10.1038/s41592-019-0686-2).
- 363 [41] Alistair A Sellar et al. “UKESM1: Description and evaluation of the UK Earth System Model”. In: *Journal*
364 *of Advances in Modeling Earth Systems* 11.12 (2019), pp. 4513–4558.
- 365 [42] D. Ackerley et al. “Regional climate modelling in New Zealand: Comparison to gridded and satellite
366 observations”. In: *Weather and Climate* 32.1 (2012), pp. 3–22. ISSN: 01115499. URL: [http://www.](http://www.jstor.org/stable/26169722)
367 [jstor.org/stable/26169722](http://www.jstor.org/stable/26169722).